



Design Principles of Synthetic Biological Oscillators

7

Ashish Panghalia and Vikram Singh

Abstract

Oscillations, having indispensable roles in the dynamics of various cellular and subcellular processes, are ubiquitous in biological systems. Construction of novel genetic oscillators is one of the key aspects of synthetic biology research. In this chapter, we have examined the underlying design principles of a variety of synthetic oscillators. We have first reviewed the oscillations in natural systems and then specified the basic characteristics of genetic oscillators. Computational methods used for the *in silico* studies of biological oscillators are described, and a list of software and tools being used is given. We have further discussed about the ten synthetic oscillators and presented a brief summary of the computational and experimental strategies involved in their realizations. This chapter is concluded by providing the hands-on exercises for numerical simulations of two synthetic oscillators.

Keywords

Genetic oscillators · Repressilator · Feedback · Deterministic simulation · Stochastic simulation · Synthetic biology

7.1 Introduction

Synthetic biology is a rapidly expanding field of research in biological sciences that aims to establish engineering rules for the forward synthesis of cellular functions (Purcell et al. 2010). Construction of the new systems, devices, and biological

A. Panghalia · V. Singh (✉)

Centre for Computational Biology and Bioinformatics, School of Life Sciences, Central University of Himachal Pradesh, Dharamshala, Himachal Pradesh, India
e-mail: vikramsingh@cuhimachal.ac.in

parts and redesigning of an existing biological system are the main thrust areas of synthetic biology. The credit of the introduction of synthetic biology research field is given to the two landmark publications: (i) genetic toggle switch (Gardner et al. 2000) and (ii) repressilator (Elowitz and Leibler 2000) that are the classic examples of artificial gene regulatory circuits, published in the beginning of the year 2000. Synthetic biology includes the combination of *in silico* and *in vitro* and sometimes *in vivo* analyses integrating the concepts of biology, mathematics, and engineering toward empowering the development of novel approaches and systematic frameworks for exploring the phenotypic behavior of a given regulatory network (Stricker et al. 2008).

Oscillations, i.e. the periodic waveform representing quantitative changes in any cyclic process (Winfree 2001), are one of the essential characteristics of all life forms and are ubiquitous in living systems. Most common routines of our life, e.g. periodic heartbeat and breathing, follow oscillatory behavior. Oscillations are observed at every time scale in biological systems, such as calcium dynamics in seconds, glycolytic oscillations in minutes, circadian clock in hours, and hormonal oscillations in days and months (Maini 1996). These oscillations are derived from several regulatory mechanisms that control the variety of dynamics occurring in living systems. The interval between two reference points in a wave signifies the time period of oscillation, which constitutes its most important feature (Winfree 2001). From the most primordial bacteria to the advanced life forms, rhythmic regulatory systems play a critical role in the emergence, evolution, and existence of life on earth. In order to capture these oscillations and understanding the science behind them, it was the need of era to develop theoretical models of these oscillatory networks. Synthetic biology aims to design the natural systems that can mimic the biological processes in order to get quantitative as well as qualitative understanding and deeper insights about the rate-limiting steps of various regulatory processes. In this chapter, we discuss biological oscillators and their existence in various forms of nature, computational and molecular approaches being employed for designing and studying these oscillations, tools and software available for exploring this concept, and the recent updates on the current state of research work in this field of science.

7.2 Oscillations in Nature

Oscillations are distributed throughout nature in one or the other form. They can exist on years' scale in the form of galactic motion or on microscopic scale as neutrino movement inside an element (Shaviv et al. 2014; Maltoni et al. 2004). The cycle of seasonal variation sheds the rays of periodicity in natural environment. Importance of these oscillations can be related to the very fundamental phenomenon of our daily life, day, and dawn (Kruse and Jülicher 2005). The cycle of day and night gives the hint that periodicity is an essential element of our life. The formation of a complete multicellular body from a single-cell "zygote" is a result of multiple cell division cycles. Heart, a vital organ in mammals, also follows rhythmic behavior generating a particular pattern of oscillations while supplying blood to various

Table 7.1 Natural biological oscillators

Biological rhythm	Approximate time period
Neural oscillations	Millisecond
Cardiac rhythms	Second
Calcium and glycolytic oscillations	Minute
Mitotic and hormonal oscillations	Hour
Circadian oscillations	Day
Menstruation cycles	Month
Circannual cycle	Years

body parts. Several regulatory mechanisms of the body, like circadian rhythms and menstrual cycle, are also common examples of biological oscillations (Karpman and Sadvovskaya 1964). The external stimuli are also important in generating frequencies in some of the biological processes. The membrane ion current is an example of such biological frequencies that occur via resonance of stereocilia present over the hair cell of inner ear (Fettiplace 2017). A variety of natural oscillators with their time scale are listed in Table 7.1.

7.3 Underlying Principles of Genetic Oscillations

Oscillation can be defined as a repetitive variation of a measure with respect to time, between two different states. Oscillations are the cyclic changes in a measurable quantity that exhibit a waveform of a relatively constant period (Winfree 2001). Oscillations are ubiquitous in nature; e.g., nervous system, heartbeat, respiration, circadian rhythms, and menstruation are all following a cyclic pattern (Cardon and Iberall 1970). In many of the cellular processes, oscillations play a vital role; such as axonemes of cilia in a cytoskeleton structure, oscillations in the concentration of Min protein play an important role in site selection for the division in some bacteria, and circadian clocks also find their basis on the genetic oscillators. The dynamic nature of cellular interacting components and their collective behavior to achieve self-organization can lead to the emergence of oscillations (Kruse and Jülicher 2005). The temporal or spatial oscillations are majorly controlled via five elements, i.e. (i) time delay, (ii) nonlinearity in regulation, (iii) negative feedback, (iv) positive feedback, and (v) noise (Cao et al. 2016).

- (i) Time delays are explained as the amount of time associated between the sensing of some disturbance and the production of a response against it. These time delays for different processes vary in a wide range. For example, various hormonal and neural activities control the rate of heartbeat and blood pressure. Every activity has an effective delay of time for response (Glass et al. 1988).
- (ii) The living systems are nonlinear in nature, which means there is no equivalent response to the external and individual inputs (Janson 2012). Nonlinearity

- in the dynamic systems gives rise to the spontaneous oscillations, which are also known as “active oscillations.” Most of the biological systems follow nonlinearity as they allow a continuous exchange of energy between the system and its surrounding environment, thus falling under this category. Biological systems generally exhibit spontaneous oscillations (Janson 2012).
- (iii) Negative feedback is observed when the output of a reaction affects its own progress in such a way so as to reduce the output. Although these negative feedback circuits are the fundamental requirement for generating oscillations, in many cases these are unable to produce oscillations on their own (Cao et al. 2016). In order to generate persistent oscillations, negative feedback loops may have to be combined with time delays or to be coupled with positive feedback loops (Cao et al. 2016).
 - (iv) The positive feedback circuit is simply a closed circuit in which output enhances the input value and vice versa (Zeigler et al. 2019) and thereby causing an increase in perturbations as a result of small disturbance on a circuit (Zeigler et al. 2019). These positive feedback loops in combination with negative feedback can generate several dynamical behaviors, like excitable pulses and bistability (Cao et al. 2016).
 - (v) Noise can be simply defined as random fluctuations (Tsimring 2014) and can affect a circuit in both, positive and negative, ways. An independent negative feedback loop is more prone to noise compared to an integrated negative–positive feedback loop (Bratsun et al. 2005). Sometimes, noise is also considered as a source of oscillations when any active feedback loop is missing (Simakov and Pérez-Mercader 2013). These elements play a vital role in modulating the oscillatory dynamics of a biological circuit, as they can enhance or damp the oscillations based on network architecture.

7.4 Computational Approaches to Study Biological Oscillations

In order to develop *in silico* models for studying the biological oscillations, the underlying biological reactions have to be developed in the form of differential equations that in turn have to be simulated to observe the emerging dynamical behavior (Singh 2015). Mathematical models can mimic the biological systems, under a given set of conditions for a defined time period. There are majorly two approaches to solve these mathematical models, i.e., deterministic and stochastic approaches. In deterministic method, the outcome of the models is completely dependent on the initial conditions and the given parameter values. Deterministic models mostly solve differential equations without introducing any random fluctuations. The output of a deterministic system is fixed if it is provided with particular input values, irrespective of the number of times it is iterated. Thus, deterministic methods model the changes in the state of a system with time as a continuous process, which can be predicted by solving coupled ODEs. In case of stochastic models, randomness is introduced, which tries to give a tint of natural systems in

mathematical models (Chandran et al. 2008). Also, deterministic models are found to have an increase in error rate with reduction in rate of reaction or lowering the protein concentration. Natural systems, generally, operate under the influence of noise resulting from random events. Therefore, in order to monitor the effect of noise on mathematical models describing a biological system, randomness is to be incorporated and such methods are known as stochastic methods (Hahl and Kremling 2016). These stochastic simulation methods, also known as Monte Carlo methods, are probability-based models. The output values of stochastic models may vary with number of iterations irrespective of same input for all simulation runs. These stochastic models consider uncertainty as an important factor in their calculations. The deterministic approach is usually taken into consideration when we expect a determined output for a specific input, but in case we have to study a system with inherent noise, most preferred method is stochastic modeling. In the following, we briefly describe the RK4 method and Gillespie's algorithms that are the two well-studied methods for deterministic and stochastic approach to solving mathematical models, respectively.

7.4.1 Runge–Kutta Method

This method is one of the well-studied methods of numerical simulations given by two German mathematicians, Carl Runge and Wilhelm Kutta, in the year 1900. The fourth order of the Runge–Kutta method also known as RK4 is generally considered as a simple and reliable numerical solution for differential equations by introducing a definite time step for a given time period. It involves the calculation of four values of slopes against the one slope calculation strategy of Euler method for solving ordinary differential equations over a range of time using a fixed value of time step. In this method, the ordinary differential equations (ODEs) are integrated by a trial time step that helps in reducing the error terms of lower order. For solving differential equation using RK4, we need to write the reaction rates in the form of ODEs for each species y under consideration with the known initial values of y , i.e. y_0 .

First-order ODEs can be constructed by further assuming the M chemical reactions, in which the N chemical species are interacting, as continuous processes.

$$\frac{dy_1}{dt} = f_1(y_1, \dots, y_n)$$

$$\frac{dy_2}{dt} = f_2(y_1, \dots, y_n)$$

$$\frac{dy_n}{dt} = f_n(y_1, \dots, y_n)$$

These equations are known as coupled rate-reaction equations, where f_i determines the rate constant of the i th chemical reaction.

In the following, we provide the basic RK4 algorithm for a single rate equation that may be extended for the coupled rate equations. Suppose, for a particular species y , $\frac{dy}{dt} = f(t, y)$ with value of y (at time t_0) = y_0 is known. This method is used to calculate the approximate value of y at given time point t , by calculating four values of slopes, as following.

$$\begin{aligned}k_1 &= h * f(t_n, y_n) \\k_2 &= h * f\left(t_n + \frac{h}{2}, y_n + \frac{k_1}{2}\right) \\k_3 &= h * f\left(t_n + \frac{h}{2}, y_n + \frac{k_2}{2}\right) \\k_4 &= h * f(t_n + h, y_n + k_3)\end{aligned}$$

where $n = 0, 1, 2, 3, \dots \left(\frac{t-t_0}{h}\right)$ and h is the step size.

$$y_{n+1} = y_n + \frac{k_1}{6} + \frac{k_2}{3} + \frac{k_3}{3} + \frac{k_4}{6} + O(h^5)$$

This calculates the value of y at next time step (y_{n+1}) from the value of y at the previous one (y_n). k_1 gives the value of increment on the basis of value of the function at the beginning, i.e. t_n . k_2 gives the value of increment on the basis of slope k_1 at the midpoint using $t_n + \frac{h}{2}$. k_3 gives the value of increment on the basis of slope k_2 at the midpoint using $t_n + \frac{h}{2}$. k_4 gives the value of increment on the basis of slope k_3 in the end using $t_n + h$.

7.4.2 Gillespie's Algorithm (Stochastic Method)

Biological processes involve the dynamics of large number of molecular events with intrinsic noise. The dynamics of such processes involve concentration of all molecules involved at nanomolar concentrations. Thus, a probabilistic model of such systems gives a closer and accurate insight about dynamics of molecular systems. D. T. Gillespie in 1977 proposed a stochastic method for simulating the effects of inherent intrinsic noise in the dynamics of systems with low molecular concentrations (Gillespie 1977). Unlike deterministic method, this algorithm is based on a single ordinary differential equation known as "Master equation" and is proposed as a solution of the "Master equation." This algorithm is derived on the basis of Monte Carlo approach to solve the dynamics of a system mathematically over a certain time period, but the time increment is not defined by definite steps.

This method attempts to solve the problem in which a fixed volume V contains the mixture of N number of different chemical species that are interacting with each other with the M number of different chemical reactions. The molecule number of each species at an initial time is given as X_i , and we have to find the population of this species at a given later time. To simulate the set of reactions that were represented as the coupled differential equations in the previous section, Gillespie's method provides the answers of two basic questions: (i) When the next reaction will occur, and (ii) Which reaction will it be? The basic methodology of the Gillespie's algorithm is described in the following schema.

- Enter the initial value of $X_i(t_0)$ for each X_i where $i = 1, 2, 3, \dots, N$ and $t_0 = 0$.
- For each reaction, enter the values of reaction probabilities c_ν , where ($\nu = 1, 2, \dots, M$).
- For each reaction, define the molecular combination functions h_ν , where ($\nu = 1, 2, \dots, M$).
- Compute the values of reaction propensities $a_\nu = h_\nu c_\nu$ where ($\nu = 1, 2, \dots, M$).
- Also calculate $a_0 = \sum_{\nu=1}^M a_\nu$.
- Using a uniform random number generator, get two random numbers r_1 and r_2 .
- Define $\tau = \left(\frac{1}{a_0}\right) \ln \left(\frac{1}{r_1}\right)$.
- Define an integer μ such that, $\sum_{\nu=1}^{\mu-1} a_\nu < r_2 a_0 \leq \sum_{\nu=1}^{\mu} a_\nu$.
- Update all the X_i according to the μ .
- Set $t = t + \tau$ and $n = n + 1$.

Value of τ gives the time interval after which a reaction will occur and μ indicates which reaction it will be. The process is to be iterated till the final time up to which simulation is to be performed.

7.5 Tools and Software to Simulate Biological Oscillations

A large number of biological systems have been studied by designing their mathematical models that can mimic the underlying dynamics of the natural system under study. Synthetic biological oscillators are, in general, designed first using a mathematical modeling approach, and the obtained results are then validated using in vitro as well as in vivo experiments. These mathematical models are composed of reaction rate equations based on the biochemical processes responsible for the emerging dynamics in the biological system under study. These equations can be solved stochastically or by converting them into ordinary differential equations (ODEs). There are various tools and software available, provided by paid and free repositories, which can be used to simulate the dynamics of these mathematical models of biological systems and to further analyze their biological significance. Few of these software and tools are listed in Table 7.2.

Table 7.2 Various tools and software for generating and analyzing the mathematical models

Name	Availability	Weblink
ASCEND	Free	http://ascend4.org/Main_Page
GNU Octave	Free	https://www.gnu.org/software/octave/
Scilab	Free	https://www.scilab.org/
Wolfram Mathematica	Free	http://www.wolfram.com/mathematica/
Simmer	Free	https://arxiv.org/abs/1705.09746
COPASI	Free	http://copasi.org/
SAGE	Paid	http://www.sageofathens.com/
XPPAUT	Free	http://www.math.pitt.edu/~bard/xpp/xpp.html
MATLAB	Paid	https://www.mathworks.com/products/matlab.html
CellDesigner	Free	http://www.celldesigner.org/
TinkerCell	Free	http://www.tinkercell.com/

7.6 A Brief Overview of the Various Synthetic Biological Oscillators

Repressilator is the first-ever-designed synthetic biological system in which oscillations were observed in the constituent protein concentrations (Elowitz and Leibler 2000). Before the realization of repressilator, there were few theoretical studies examining the onset of oscillations in biological systems that provided the basis for understanding the underlying basic concepts for successful realization of a synthetic oscillator, such as synthetic genetic oscillator by Goodwin in 1965 (Goodwin 1965), genetic feedback repressor solved using Boolean modeling by Fraser in 1974 (Fraser and Tiwari 1974), molecular basis of periodic cellular rhythms by Goldbeter in 1997 (Goldbeter 1997), and two-gene oscillator by Smolen in 1998 (Smolen et al. 1998). In approximately 20 years of post repressilator synthetic biology research, significant work is done in the development and understanding of synthetic biological oscillators. In the following, we provide a brief summary of ten synthetic oscillators.

7.6.1 Goodwin Oscillator

Goodwin oscillator (Goodwin 1965) is known as the first synthetic genetic oscillator that was proposed with a theoretical model and studied computationally over 50 years ago. In this model, there is only one gene that represses the expression of itself as shown in Fig. 7.1a.

L_i represents the gene locus transcribing mRNA (denoted by X_i) that in combination with the ribosome forms polysome (R) that helps in the production of its proteins (Y_i). The protein formed is assumed as an enzyme that helps in the metabolic transformation and gives rise to the metabolic species M_i that in turn

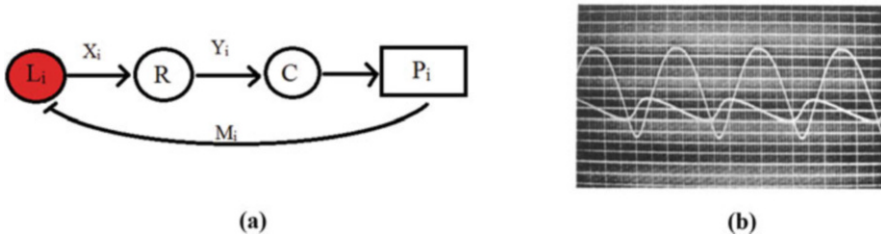


Fig. 7.1 (a) Topology of single-gene oscillator, which represses itself. (b) Simulation results of the Goodwin oscillator. Figure (b) reproduced with permission from Goodwin (1965) © (1965) Elsevier Ltd

lowers down the expression of gene (L_i) by repressing it. Following equations give the dynamics of this system.

$$\frac{dX_i}{dt} = \frac{a_i}{A_i + k_i Y_i} - b_i$$

$$\frac{dY_i}{dt} = \alpha_i X_i - \beta_i$$

Here, X_i represents the concentration of mRNA and Y_i represents the concentration of protein. The oscillations produced from the numerical simulations of these equations are shown in Fig. 7.1b.

7.6.2 Smolen's Oscillator

Smolen's oscillator (Smolen et al. 1998) is a simple kinetic model that examines the dynamic activity of the gene regulatory systems including autoregulation, phosphorylation, and dimerization of transcription factors along with noise and feedback. There are two genes in this oscillator. The first gene (A) promotes the transcription of second gene (B) and also its own transcription, and the second gene represses the transcription of first gene as well as its own transcription as shown in Fig. 7.2a.

In this model, signal-transduction pathway was considered in which stimuli leads in the formation of the homodimer and the phosphorylation of TFs, those bind with the specific responsive-element DNA sequences (TF-REs). Dimer of phosphorylated TF-A protein binds to TF-RE and activates the transcription of *tf-a* and *tf-r* genes which forms the TF-A and TF-R proteins. The rate constants for degradation of TF-A and TF-R are represented by $k_{1,d}$, and $k_{2,d}$ respectively. TF-R protein represses the transcription of the *tf-r* gene by binding to TF-RE, whereas it represses the transcription of the *tf-r* gene by competitively inhibiting the binding of TF-A to TF-RE as shown in Fig. 7.2b.

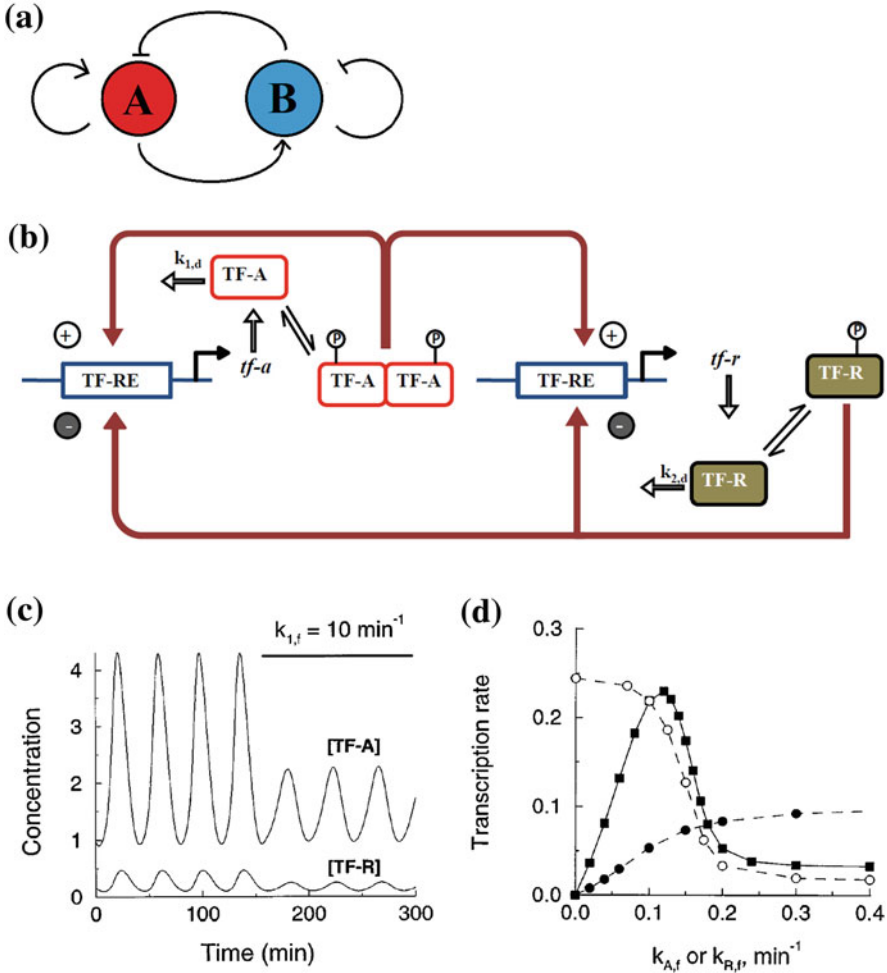


Fig. 7.2 (a) Topology of Smolen's oscillator. (b) Schematic representation of the Smolen's oscillator. (c) Oscillations obtained by the numerical simulations of the Smolen's oscillator. (d) Oscillations obtained in the experimental conditions. Figures (b), (c), (d) are adopted from Smolen et al. (1998)

7.6.2.1 ODEs for the In Silico Implementation of Smolen's Oscillator

Here, $K_{R,d}$ represents the dissociation constant of TF-R from TF-REs. $k_{1,f}$, and $k_{2,f}$ are the maximal synthesis rates. $k_{1,d}$ and $k_{2,d}$ are the rate constants of degradation, and $K_{2,d}$ represents the dissociation constant of TF-A from TF-REs.

$$\frac{d[TF-A]}{dt} = \frac{k_{1,f}[TF-A]^2}{[TF-A]^2 + K_{1,d}(1 + [TF-R]/K_{R,d})} - k_{1,d}[TF-A] + r_{1,bas}$$

$$\frac{d[TF - R]}{dt} = \frac{k_{2,f}[TF - A]^2}{[TF - A]^2 + K_{2,d}(1 + [TF - R]/K_{R,d})} - k_{2,d}[TF - R]$$

$r_{1, \text{bas}}$ gives the basal rate due to which an activator is synthesized at a negligible concentration of dimer. $k_{1,d}$ gives the rate constant of the first-order degradation of TF-A. Oscillations were readily generated by this model as shown in Fig. 7.2c.

7.6.3 Repressilator

The theoretical framework of repressilator was developed in 1974, using discrete Boolean simulations as an extension of the Goodwin's oscillator (Fraser and Tiwari 1974). It may be explained as a regulatory network of three genes, in which each gene represses the expression of its successor gene in a cyclic manner (Elowitz and Leibler 2000). LacI protein from *Escherichia coli* inhibits the transcription of the TetR gene. The expression of cI gene from λ phage is inhibited by the second repressor protein named TetR of Tn10 transposon. Finally, cI which is the third repressor protein inhibits the transcription of LacI gene and completes the cycle shown in Fig. 7.3a, b.

7.6.3.1 ODEs for the In Silico Implementation of Repressilator

Following six-coupled first-order differential equations determine the dynamics of this system. Here, p_i represents the concentration of repressor proteins and m_i represents the concentration of their corresponding mRNAs. Each of these is considered as the continuous dynamic variables (i is LacI, TetR, and cI, respectively).

$$\frac{dm_i}{dt} = -m_i + \frac{\alpha}{(1 + p_j^n)} + \alpha_0$$

$$\frac{dp_i}{dt} = -\beta(p_i - m_i) \quad \begin{pmatrix} i = l < \text{cI, tetR, cI} \\ j = \text{cI, lacI, tetR} \end{pmatrix}$$

Where, α_0 gives the protein copy number produced by a given promoter type in each cell when the saturated amount of repressor is present and $\alpha + \alpha_0$ is the protein copies when the repressor is absent. The ratio of decay rates of protein to mRNA is denoted by β and n is the Hill coefficient. Using these six coupled differential equations corresponding to three mRNAs and their repressor proteins, oscillations were obtained by in silico ODEs simulation as shown in Fig. 7.3c that were also successfully reproduced in the in vitro experiments shown in Fig. 7.3d.

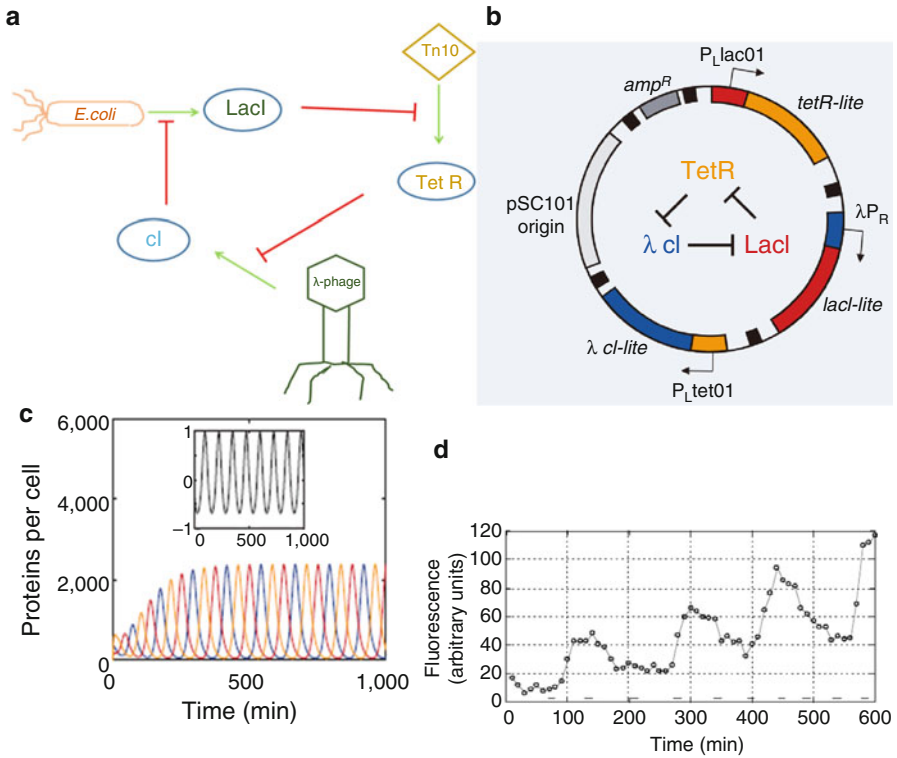


Fig. 7.3 (a) Topology of repressilator in which the every gene represses the transcription of its successor. (b) Repressilator network. (c) Simulations of ODEs of repressilator genes. (d) Oscillation shown in living bacteria. Figures (b), (c), (d) are reproduced with permission from (Elowitz and Leibler 2000) © (2000) Macmillan Magazines Ltd

7.6.4 Genetic Relaxation Oscillator

The topology of this oscillator consists of various nodes that were linked with the activating and repressing links Chaos (Hasty et al. 2001). The transcription of gene A and gene B is upregulated by gene A at the lower concentration of its protein. The transcription of the first gene (A) and second gene (B) is regulated by gene A via variable promoter, and the transcription of gene A is repressed by gene B via degradation as shown in Fig. 7.4a.

There are two plasmids which are used to control the repressor (X) and RcsA (Y) production by using the P_{RM} promoter as shown in Fig. 7.4b. Both the plasmids are turned on by the activity of repressor at P_{RM} . The concentration of RcsA starts increasing as the promoter gets activated, which leads to the reduction of the concentration of repressor.

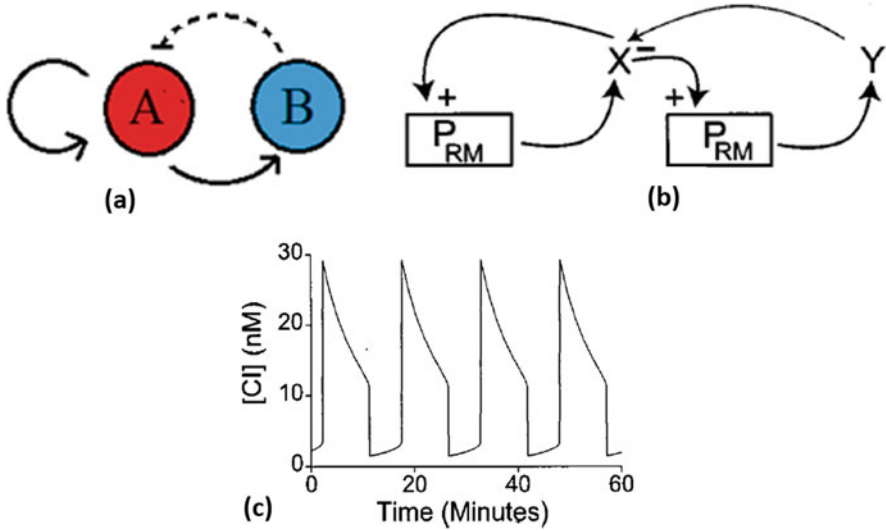


Fig. 7.4 (a) Topology of amplified variable link oscillator. (b) Working of amplified variable link oscillator. (c) Simulation generated for amplified variable link oscillator. Figures (b), (c) are reproduced with permission from Hasty et al. (2001) © (2001) American Institute of Physics

7.6.4.1 ODEs for the In Silico Implementation of Genetic Relaxation Oscillator

In the given equations, x and y represent the quantity and m_x and m_y are the copy numbers of the plasmid of cI and RcsA, respectively.

$$\frac{dx}{dt} = m_x f(x) - \gamma_x x - \gamma_{xy} x y$$

$$\frac{dy}{dt} = m_y f(x) - \tilde{a}_y y$$

γ_x and γ_y represent the degradation of cI and RcsA and γ_{xy} shows the degradation rate of cI by RcsA. Simulations of the ODEs give the oscillations as shown in Fig. 7.4c.

7.6.5 Amplified Negative Feedback Oscillator

The previously studied oscillators, like the Goodwin oscillator and repressilator, were based on the negative feedback cycle only. The amplified negative feedback oscillator (Atkinson et al. 2003) was proposed to showcase the usage of positive feedback loops in the expression of oscillations. It comprises two genes (A and B): one gene (A) activates the self-transcription via positive feedback and also promotes

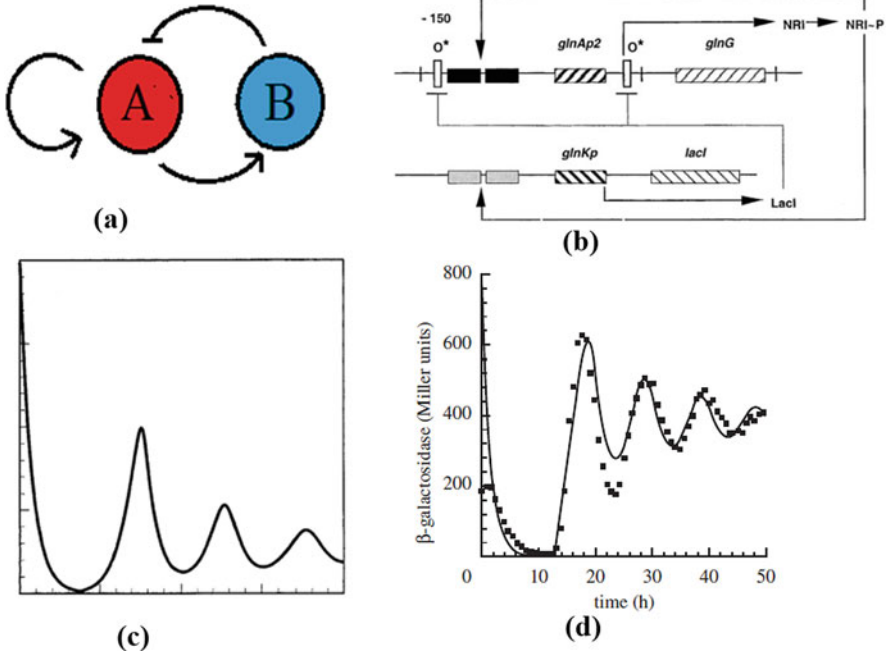


Fig. 7.5 (a) Topology of amplified negative feedback oscillator. (b) Schematic working of amplified negative feedback oscillator. (c) Simulation generated for amplified negative feedback oscillator. (d) Dynamics obtained in the experimental conditions. Figures (b), (c), (d) are reproduced with permission from Atkinson et al. (2003) © (2003) Cell Press

the transcription of the second gene (B). Simultaneously, the transcription of the first gene is repressed by the second gene as shown in Fig. 7.5a.

7.6.5.1 ODEs for the In Silico Implementation of Amplified Negative Feedback Oscillator

The concentrations of various components of a network are represented by x_i , and the concentrations of proteins and mRNAs are represented by the even and odd-numbered variables, respectively.

$$\frac{dx_{(2k-1)}}{dt} = \beta_{(2k-1)} (f_{(2k-1)} - x_{(2k-1)})$$

$$\frac{dx_{(2k)}}{dt} = \beta_{2k} (x_{2k-1} - x_{2k}) \text{ for } k = 1, 2, \quad (3)$$

Here, f_i (transcriptional rate of three phases) and β_i (numerous rates which describe constants) are described by the two equations. There are two modules in this network: one is NRI that encodes the activator and second is LacI that encodes the repressor. Encoding NRI is fused with *glnG* to the control region on the promoter of *glnA* as shown in Fig. 7.5b to construct the module which acts as an activator to the oscillator. The regulation of promoter was done in the presence of two phosphorylated NRI-binding sites (NRIp) which are upstream to the promoter and form enhancer, and two LacI operators one of which is present downstream of promoter and other is upstream of enhancer. The oscillations are obtained by in silico ODEs simulation as shown in Fig. 7.5c.

7.6.6 Metabolator

Metabolator (Fung et al. 2005) is reported as the first oscillator in which along with the genes, metabolites also constitute the main components of its circuitry. It consists of two genes (A and B), gene B produces an enzyme which can convert one metabolic pool named M2 to another pool named M1 and the transcription of this gene B is also activated by M2. At the same time, another enzyme is produced by the gene A which enables the conversion of the M1 pool to the M2 pool, and the M2 represses the transcription of this gene A. Moreover, there is an influx and efflux from the M1 and M2 pools, respectively, as shown in Fig. 7.6c. The topology of this oscillator (metabolator) is schematically represented in Fig. 7.6b as a gene regulatory network.

Gene A and B repress themselves by activating the M2 and also activate each other as shown in Fig. 7.6b. This concept was implemented by modeling with ODEs and Chemical Langevin Equations (CLEs) which represent a GFP reporter (Fung et al. 2005). Due to an increase and decrease in the M2 pool, the two genes repress their activity as a result of which these two genes regulate the activity of each other.

7.6.6.1 ODEs for the In Silico Implementation of Metabolator

$$\frac{d \text{AcCoA}}{dt} = V_{\text{Acs}} - V_{\text{Pta}} - V_{\text{gly}} - V_{\text{TCA}}$$

$$\frac{d \text{AcP}}{dt} = V_{\text{Pta}} - V_{\text{Ack}}$$

$$\frac{d \text{OAc}^-}{dt} = V_{\text{Ack}} - V_{\text{AcE}} - V_{\text{Acs}}$$

$$\frac{d \text{HOAc}}{dt} = V_{\text{AcE}} - V_{\text{out}}$$

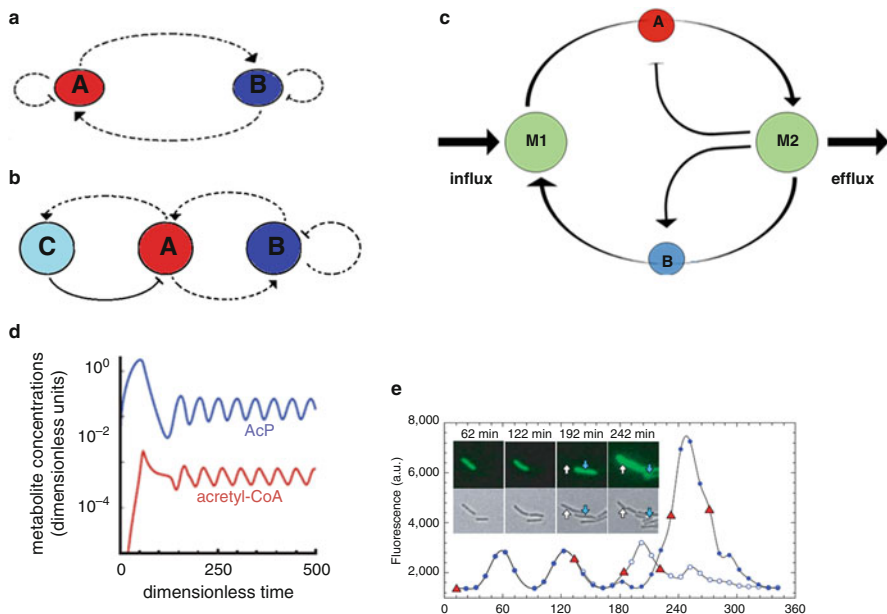


Fig. 7.6 (a) Schematic GRN diagram and (b) topology of metabolator. (c) Conceptual view of metabolator. (d) In silico simulations in high glycolytic flux. (e) Fluorescence trajectory of single cell. Figures (d), (e) are reproduced with permission from Fung et al. (2005) © (2005) Nature Publishing Group

The concentration of three key proteins was determined by:

$$\frac{d \text{LacI}}{dt} = R_{\text{LacI}} - R_{d,\text{LacI}}$$

$$\frac{d \text{Pta}}{dt} = R_{\text{Pta}} - R_{d,\text{Pta}}$$

$$\frac{d \text{Acs}}{dt} = R_{\text{Acs}} - R_{d,\text{Acs}}$$

The mathematical analysis showed that the oscillations as shown in Fig. 7.6d were produced through a Hopf bifurcation. Here, V_i represents the expression of rate of reaction of Glycolytic flux (V_{gly}), Acs flux (V_{Acs}), Pta flux (V_{Pta}), flux to TCA (V_{TCA}), flux for the AcP and OAc^- reaction (V_{Ack}), equilibrium of acid base for acetic acid (V_{AcE}), HOAc transport rate (V_{out}), and R_{LacI} , R_{Pta} , R_{Acs} , represent the synthesis rate of LacI, Pta, and Acs, respectively. R_d ($X = \text{LacI}$, Pta, and Acs) represents the degradation rate of LacI, Pta, and Acs. It was observed that for the presence of oscillations, a high inflow rate is required which can be abolished by the high concentration of M2. The number of relative gene copies has also affected the

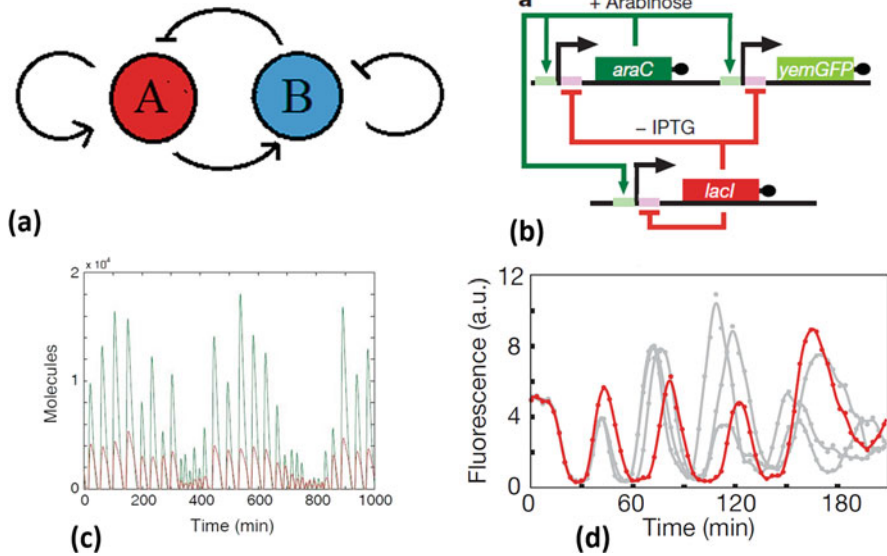


Fig. 7.7 (a) Topology of Hasty's two-gene oscillator. (b) Schematic working of Hasty's two-gene oscillator. (c) Bistable oscillations generated for Hasty's two-gene oscillator. (d) Experimental fluorescence trajectories of single cell. Figures (b), (c), (d) are reproduced with permission from Stricker et al. (2008) © (2008) Macmillan Publishers Limited

production of oscillations, while the amplitude variation created by the addition of noise is found by the CLE simulations.

7.6.7 Two Genes Based Oscillator

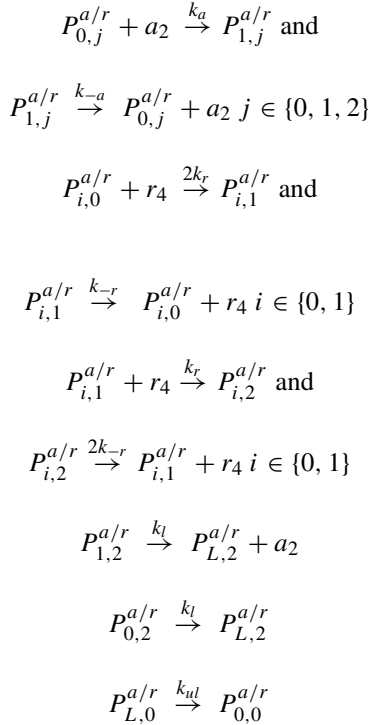
This oscillator (Stricker et al. 2008) contains two genes as shown in Fig. 7.7a. Gene A, which is the first gene, promotes itself and also of the second gene. Gene B, the second gene, represses itself and also the transcription of gene A. This tendency of self-repression in gene B is the major factor which makes the difference between the topology of Hasty's two-gene oscillator and amplified negative feedback oscillator.

E. coli components were used for the development of this oscillator consisting of a hybrid promoter named as Plac/ara-1, which constitutes the araBAD promoter's activation operator site which is placed in its start site, and lacZYA promoter's repression operator site and placed to the upstream end and downstream end of the start site. AraC protein helps in activation when arabinose is present, and LacI protein acts as a repressor when isopropyl b-D-1-thiogalactopyranoside (IPTG) is absent.

Three co-regulated transcription modules were formed by placing the *araC*, *lacI*, and *yemGFP* (monomeric yeast-enhanced green fluorescent protein) genes that are controlled by three identical copies of the promoter *Plac/ara-1*. When arabinose and IPTG are added, it activates the promoter which causes the transcription of each component and the presence of arabinose results in the increase of AraC, which corresponds to a positive feedback loop due to which the activity of the promoter gets increased. At the same time, promoter activity gets decreased due to the increased production of LacI, which results in the formation of linked negative feedback loop as shown in Fig. 7.7b. The oscillatory behavior can be driven by the differential activity of these two feedback loops (Stricker et al. 2008).

7.6.7.1 Modeling of Two-Gene Oscillator Using the Stochastic Approach

The dynamics of the promoter is based on the following equations.



Here, $P_{0,j}^{a/r}$ shows the status of the promoter on the plasmid of activator (a) and repressor (r) with AraC dimer (a_2) and LacI tetramer (r_4) bound. Where $i \in \{0, 1\}$ and $j \in \{0, 1, 2\}$. In the next step, the set of reaction is for the transcription, translation, folding of protein, and multimerization of each gene and protein. Due

to the space constraints, all the reactions are not given here. Interested readers may find the detailed reactions in the supplementary file of original article (Stricker et al. 2008).

7.6.8 Mammalian Oscillators

This is an oscillator (Tigges et al. 2009) that is executed in the eukaryotic system to understand their regulatory mechanism, which consists of an expression unit of sense–antisense that encodes for the tetracycline-dependent transactivator (tTA) that is triggered by pristinamycin-dependent transactivator (PIT) as shown in Fig. 7.8c. It comprises two genes: gene A and gene B from which both sense and antisense transcriptions occur from one of the gene. The protein is formed due to the translation of sense transcript which results in the feedback to itself along with the activation of the second gene (B). The translation of the antisense transcript from the first gene (A) is activated by the second gene (B). The transcript is not translated to protein, but it represses the production of sense protein at the translational level,

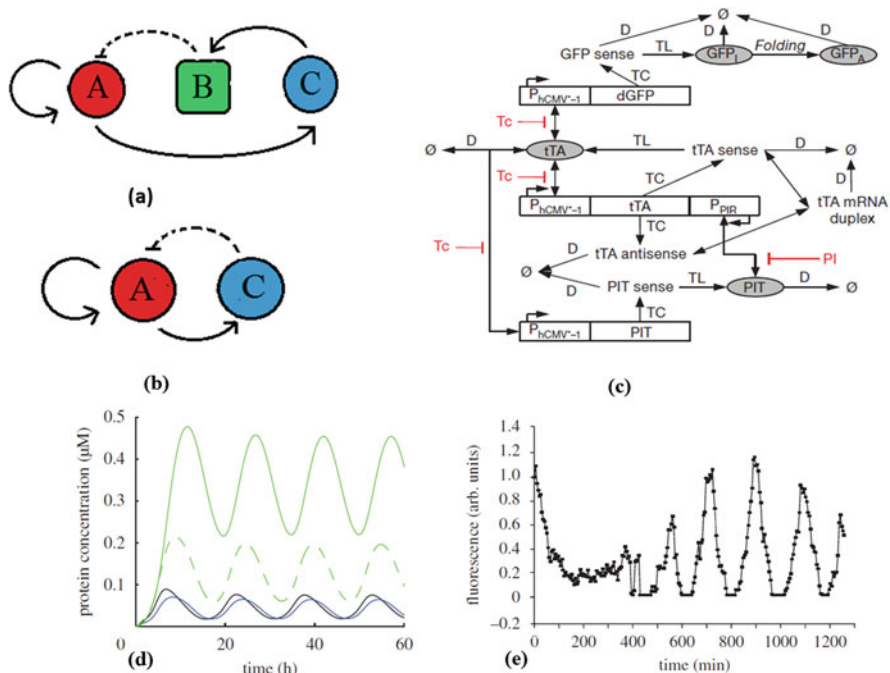


Fig. 7.8 (a) Topology of oscillator and (b) oscillator as an example of amplified negative feedback topology. (c) A cellular process considered for the mathematical model. (d) Simulation results of the ODEs of Fussenegger oscillators. (e) Oscillations of the oscillator as observed by the time lapse fluorescence analysis. Figures (c), (d), (e) are reproduced with permission from Tigges et al. (2009) © (2009) Macmillan Publishers Limited

due to which negative feedback loop is completed as shown in Fig. 7.8a. Therefore, this Fussenegger oscillator is also a type of amplified negative feedback oscillator, shown in Fig. 7.8b. Moreover, there are delays in the repressive effect which are the extra step involved in a negative feedback loop. ODEs and Gillespie simulations were used for the implementation of this oscillator. These models examined the interaction of RNA polymerases that transcribe the sense and antisense transcripts, which may act as an important repercussion to the repression of sense–antisense strands. After many improvement rounds, a final model is generated by the extensive parameter estimation of data from in vivo analysis.

7.6.8.1 ODEs for the In Silico Implementation of Oscillator

The model is generated by considering the production and degradation of tTA and PIT. The ODEs for the system are written as follows:

$$\frac{dT_m}{dt} = G_1 \cdot r_T - k_1 A_m T_m + AT_m \cdot (k_2 k_{DA_m}) - k_{DT_m} T_m$$

$$\frac{dT_p}{dt} = k_{TL} \cdot T_m - k_{DT_p} \cdot T_p$$

$$\frac{dP_m}{dt} = G_2 \cdot r_T - k_{DP_m} \cdot P_m$$

$$\frac{dP_p}{dt} = k_{TL} \cdot P_m - k_{DP_p} \cdot P_p$$

$$\frac{dA_m}{dt} = G_1 \cdot r_P - k_1 A_m T_m + AT_m \cdot (k_2 k_{DT_m}) - k_{DA_m} A_m$$

$$\frac{dAT_p}{dt} = k_1 \cdot A_m \cdot T_m - AT_m \cdot (k_2 + k_{DT_m} + k_{DA_m})$$

$$\frac{dG_m}{dt} = G_3 \cdot r_T - k_{DG_m} \cdot G_m$$

$$\frac{dG_p}{dt} = k_{TL} \cdot G_m - (k_3 + k_{DG_p}) \cdot G_p$$

$$\frac{dG_a}{dt} = k_3 \cdot G_p - k_{DG_p} \cdot G_a$$

In the given ODEs, T_m is the concentration of mRNA of tTA, T_p is the concentration of protein of tTA, P_m is the mRNA concentration of PIT, P_p is the protein concentration of PIT, A_m is the antisense mRNA of tTA, TA_m is the complex of sense–antisense mRNA, G_m is the GFP in mRNA, G_p and G_a represent the inactive and active GFP, respectively.

7.6.9 Two-Switch Negative Feedback Oscillator

This oscillator (Kim and Winfree 2011) consists of two switches both consisting of a synthetic DNA (each having a regulatory domain, a promoter region, and an output domain), inhibitory molecule, and an activator. An input signal controls these synthetic switches. These switches operate at a particular threshold in response to the input signal of the respective switch. These responses derive from the different hybridization of DNA and RNA molecules, i.e. activation, inhibition, annihilation, and release. The OFF switch consists of a double-stranded DNA having an incomplete promoter region for RNA polymerase as shown in Fig. 7.9b. When a

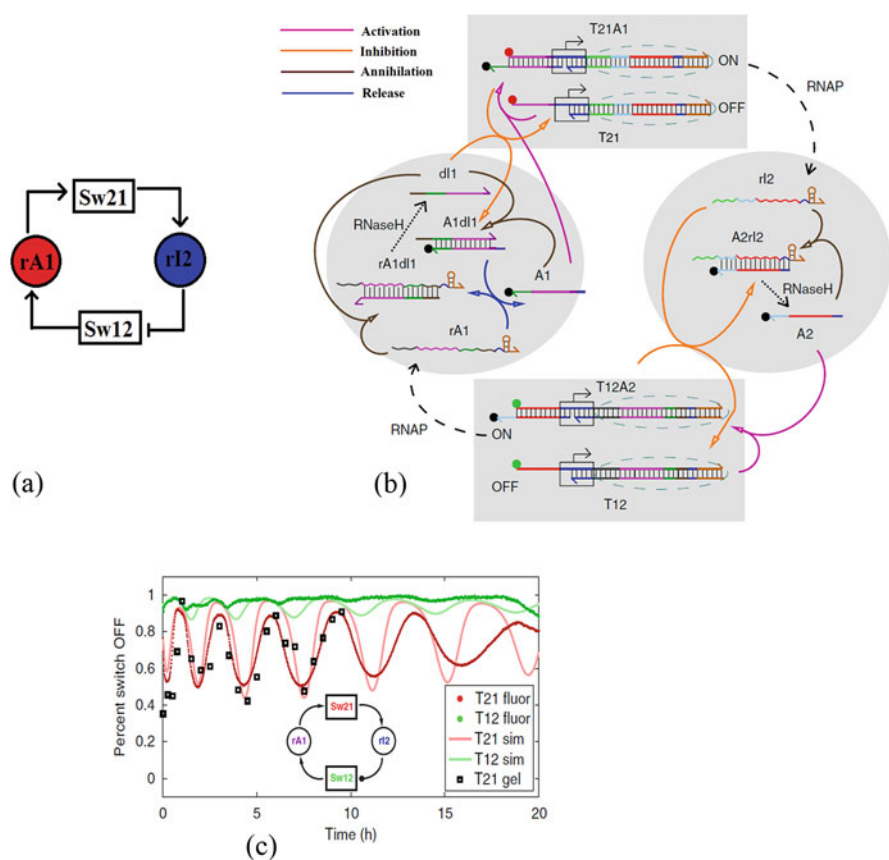


Fig. 7.9 (a) Topology of two-switch negative feedback oscillator. (b) Schematic circuit diagrams of two-switch negative feedback oscillator. (c) Oscillation observed by fluorescence analysis. Figures (b), (c) are adopted from Kim and Winfree (2011) © (2011) EMBO and Macmillan Publishers Limited

single-stranded DNA activator (A) binds to the DNA molecule, it completes the promoter region due to which this switch gets ON (*activation*). An inhibitor strand of either single-stranded DNA (dI) or single-stranded RNA (rI) molecule can bind to the free floating activators of either single-stranded DNA (A) or single-stranded RNA (rA) that are complementary to the inhibitors resulting in the formation of the activator-inhibitor complex which is functionally inactive (*annihilation*). The free activator strands can reduce the inhibitory strands concentration resulting in the availability of only that strand which had high initial concentration. On the addition of inhibitory strands, if the amount of inhibitory strands rises above the amount of free activators, the switch gets OFF (*inhibition*). There is a toehold region of DNA inhibitor (dI) on A.dI complex that allows the binding of RNA activator (rA) releasing the DNA activator (A) to activate the target switch (*release*) due to the toehold-mediated strand displacement reaction. An inhibitable switch or an activatable switch is formed by assembly of the four hybridization reactions on the basis of the concentration of DNA inhibitor or activator strand.

7.6.9.1 ODEs for the In Silico Implementation

$$\frac{d[rA1]}{dt} = k_p \cdot [T12A2] - k_d \cdot [rA1]$$

$$\frac{d[rI1]}{dt} = k_p \cdot [T21A1] - k_d \cdot [rI1]$$

Here, k_p and k_d are the rate constants of the RNAP and RNaseH, respectively. A change in state of switches is governed by the hybridization reactions depending on the amount of presence of the amount of X. The steady-state response of a switch to the RNA input can be approximated by Hill functions.

$$\tau \frac{d[T12A2]}{dt} = [T12^{\text{tot}}] \left(\frac{1}{1 + \left(\frac{[rI1]}{K_I} \right)^n} \right) - [T12A2]$$

$$\tau \frac{d[T21A1]}{dt} = [T21^{\text{tot}}] \left(\frac{1}{1 + \left(\frac{[rA1]}{K_A} \right)^n} \right) - [T21A1]$$

Where, n and m represent the Hill exponents, τ shows the relaxation time for the hybridization reaction, and K_A and K_I represent the threshold set by the DNA activator and DNA inhibitor, respectively. T_{ij} represents the sum of the concentrations of ON-state switch $[T_{ij}A_j]$ and OFF-state switch $[T_{ji}A_i]$, and $T21^{\text{tot}}$ gives the sum of all the concentrations of species of $[T_{ij}A_j]$ and $[T_{ji}A_i]$. We

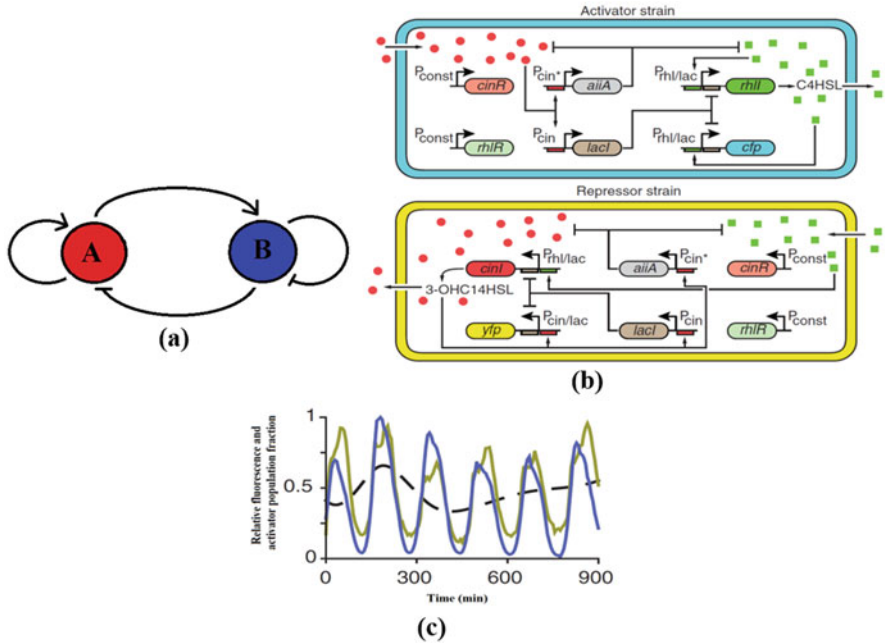


Fig. 7.10 (a) Topology of the dual-feedback consortium oscillator. (b) Circuit diagrams of both the activator and repressor strains of the dual-feedback consortium oscillator. (c) Oscillations observed in fluorescence analysis. Figures (b), (c) are adopted from Chen et al. (2015) © (2015) AAAS

are omitting the details of the other equations because of the space constraints. Furthermore, positive-feedback loop was also added to study the modularity, and a ring oscillator having three switches was developed and analyzed (Kim and Winfree 2011).

7.6.10 Dual-Feedback Consortium Oscillator

This oscillator was designed primarily to address the challenge of developing a microbial system which shows the population-level behaviors in synthetic biology using the mechanisms of cell signaling for regulation of gene expression. This consortium consists of two different types of cells: activator strain (A) and repressor strain (B) (Chen et al. 2015). Both of these cell types produce two distinct cell-signaling molecules as shown in Fig. 7.10b. These molecules regulate the gene expressions in the cells of both types of strains. The population-level oscillations were produced by these two strains when they were cultured together.

In this model, a signaling molecule C4–homoserine lactone (C4-HSL) is produced by the activator strain which enhances the rate of transcription of *rhII* and *cfp* genes, regulated by the different copies of hybrid promoter $P_{rhI/lac}$, and also enhances the rate of transcription of target gene in repressor strain. Whereas in the repressor strain, 3-OHC14-HSL is produced as a signaling molecule which inhibits the transcription of *cinI* (regulated by $P_{rhI/lac}$) and *rhIR* regulated by $P_{cin/lac}$ as well as represses the target genes in repressor strains by production of repressor LacI as shown in Fig. 7.10b. A coupled negative–positive feedback loop is formed by the two signaling molecules formation mechanisms when these two strains were grown with each other. Furthermore, an enzyme AiiA is produced when both strains were active, which inhibits the formation of both of the signaling molecules.

7.6.10.1 ODEs for the In Silico Implementation of Dual-Feedback Consortium Oscillator

Here, F_a and Y_r represent the productions of reporter proteins CFP and YFP, respectively. The F_a production and Y_r productions are directly proportional to the $P_{rhI/lac}$ and $P_{cin/lac}$ promoter's activity, respectively.

$$\frac{dF_a}{dt} = \frac{\eta_{F0} + \eta_{F1} (H_a^\tau / K_H)^{n_H}}{1 + (H_a^\tau / K_H)^{n_H} + (L_a^\tau / K_L)^{n_L}} + \frac{d_C F_a}{K_C + R_a + A_a + L_a + F_a + M_a} - dF_a - mF_a$$

$$\frac{dM_a}{dt} = mF_a - \frac{d_C F_a}{K_C + R_a + A_a + L_a + F_a + M_a} - dM_a$$

$$\frac{dY_r}{dt} = \frac{\eta_{Y0} + \eta_{Y1} (I_r^\tau / K_I)^{n_I}}{1 + (I_r^\tau / K_I)^{n_I} + (L_r^\tau / K_L)^{n_L}} + \frac{d_C Y_r}{K_C + R_r + A_r + L_r + Y_r + M_r} - dY_r - mY_r$$

$$\frac{dM_r}{dt} = mY_r - \frac{d_C M_r}{K_C + R_r + A_r + L_r + Y_r + M_r} - dM_r$$

M_a represents the mature CFP, and M_r represents the mature YFP, which is described by first-order reaction. η_{F0} and η_{F1} show the basal and final rates of production of CFP, where η_{Y0} and η_{Y1} show the basal and final rates of production of YFP. The rate of production of C4-HSL and 3-OHC14-HSL is given by H_a and I_r , respectively. τ represents the time delay. K_H and K_L represent the EC50 of C4 and IC50 for LacI, respectively. n_H is the Hill-coefficient of C4, and n_L is the Hill-coefficient of LacI. Due to space constraints, we are not detailing here the complete set of equations. Interested researchers may find the details in the original research article describing the construction and realization of this consortium (Chen et al. 2015).

7.7 Hands-On Exercises

In order to practice the simulation of synthetic oscillators, two exercises (using XPPAUT software in a windows machine) are given below in a step-by-step manner.

For that, we need to first download and install XPPAUT following instructions given in <http://www.math.pitt.edu/~bard/xpp/xpp.html>. Downloaded folder is to be unzipped and to be copied into C:/ drive. One needs to install an X-Window System Server also, if not preinstalled. Xming is one such server that can be installed from <https://sourceforge.net/projects/xming/>. Input file for the XPPAUT is to be developed as given in the following format and to be saved with an .ode extension.

7.7.1 Sample .ode File for Simulating the Dynamics of Goodwin's Oscillator

$$\frac{dx}{dt} = \left(\frac{a}{(S + k * y)} \right) - b$$

$$\frac{dy}{dt} = (a1 * x) - b1$$

param $a = 72, S = 36, k = 1, b = 2, a1 = 1, b1 = 0$

init $x = 7, y = -10$

done

7.7.2 Sample .ode File for Simulating the Dynamics of Repressilator

$$\frac{dm_1}{dt} = -m_1 + \frac{a}{(1 + p_3 \hat{n})} + a_1$$

$$\frac{dp_1}{dt} = -b * (p_1 - m_1)$$

$$\frac{dm_2}{dt} = -m_2 + \frac{a}{(1 + p_1 \hat{n})} + a_1$$

$$\frac{dp_2}{dt} = -b * (p_2 - m_2)$$

$$\frac{dm_3}{dt} = -m_3 + \frac{a}{(1 + p_2 \hat{n})} + a_1$$

$$\frac{dp_3}{dt} = -b * (p_3 - m_3)$$

#parameters

param a = 10, a₁ = 0.01, b = 0.2, n = 2

#initial conditions

init m₁ = 0.2, m₂ = 0.3, m₃ = 0.4, p₁ = 0.1, p₂ = 0.1, p₃ = 0.5

@bound = 10,000

done

The above given file contains all the differential equations of Goodwin's oscillator and repressilator, initial conditions (init), parameters (param), time step (dt), total run time (total), xplot (x-axis), and yplot (y-axis).

7.7.2.1 Steps for Running the Input Files Using XPPAUT

- Copy the shortcut of XPPAUT to the desktop.
- Run the XMING.
- Drag your file "*.ode" to the shortcut. This will open the file in XPPAUT.
- Set your x-axis from xi vs t option.
- Set your initial run conditions from InitialConds > Range option.
- Go to Window/zoom option and choose fit to see the dynamics.

Once run, one should get the dynamics of Goodwin's oscillator and repressilator, as shown in the Figs. 7.11a, b, respectively.

Acknowledgement AP thanks University Grants Commission, India, for providing PhD fellowship.

Conflict of Interest The authors declare that they have no conflict of interest.

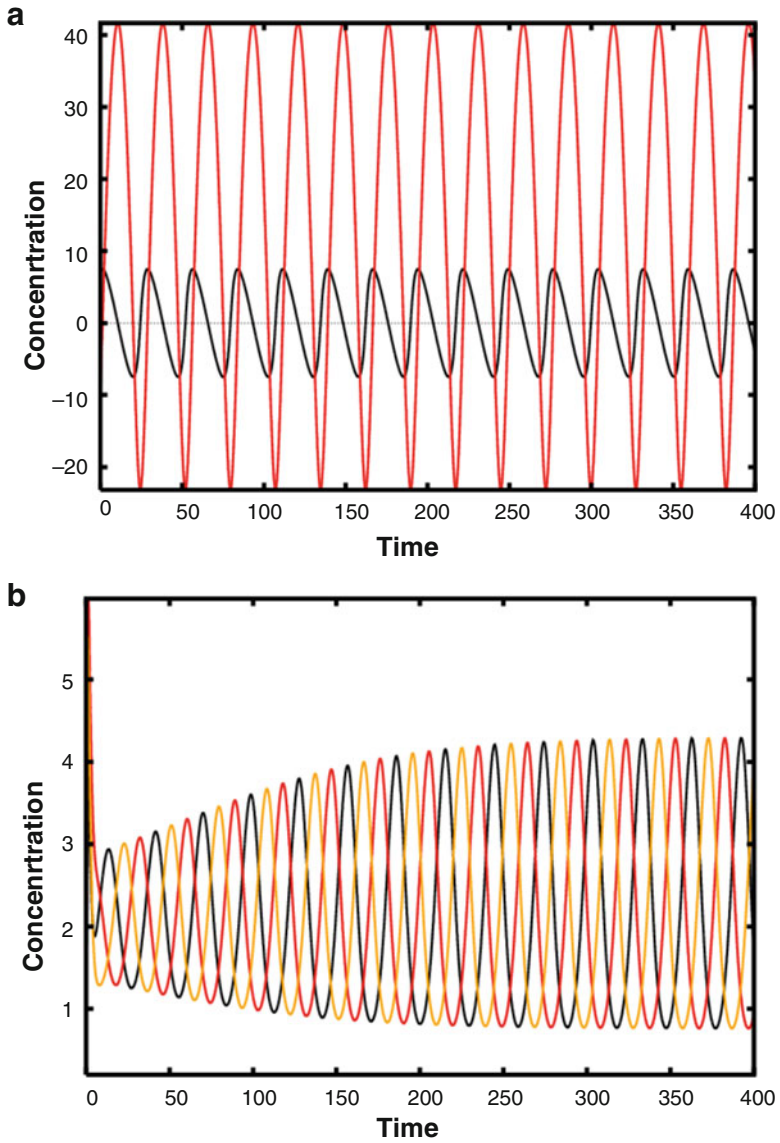


Fig. 7.11 (a) Dynamics of Goodwin's oscillator and (b) dynamics of repressilator

References

- Atkinson MR, Savageau MA, Myers JT, Ninfa AJ (2003) Development of genetic circuitry exhibiting toggle switch or oscillatory behavior in *Escherichia coli*. *Cell* 113(5):597–607
- Bratsun D, Volfson D, Tsimring LS, Hasty J (2005) Delay-induced stochastic oscillations in gene regulation. *Proc Natl Acad Sci USA* 102(41):14593–14598
- Cao Y, Lopatkin A, You L (2016) Elements of biological oscillations in time and space. *Nat Struct Mol Biol* 23:1030–1034
- Cardon SZ, Iberall AS (1970) Oscillations in biological systems. *Biosystems* 3(3):237–249
- Chandran D, Copeland WB, Sleight SC, Sauro HM (2008) Mathematical modeling and synthetic biology. *Drug Discov Today Dis Model* 5(4):299–309
- Chen Y, Kim JK, Hirning AJ, Josić K, Bennett MR (2015) Emergent genetic oscillations in a synthetic microbial consortium. *Science* 349(6251):986–989
- Elowitz MB, Leibler S (2000) A synthetic oscillatory network of transcriptional regulators. *Nature* 403(6767):335–338
- Fettiplace R (2017) Hair cell transduction, tuning, and synaptic transmission in the mammalian cochlea. *Compr Physiol* 7(4):1197–1227
- Fraser A, Tiwari J (1974) Genetical feedback-repression II. Cyclic genetic systems. *J Theor Biol* 47(2):397–412
- Fung E, Wong WW, Suen JK, Bulter T, Lee S, Liao JC (2005) A synthetic gene-metabolic oscillator. *Nature* 435:118–122
- Gardner TS, Cantor CR, Collins JJ (2000) Construction of a genetic toggle switch in *Escherichia coli*. *Nature* 403(6767):339–342
- Gillespie DT (1977) Exact stochastic simulation of coupled chemical reactions. *J Phys Chem* 81(25):2340–2361
- Glass L, Beuter A, Larocque D (1988) Time delays, oscillations, and chaos in physiological control systems. *Math Biosci* 90:111–125
- Goldbeter A (1997) Modelling biochemical oscillations and cellular rhythms. *Curr Sci* 73(11):933–939
- Goodwin BC (1965) Oscillatory behavior in enzymatic control processes. *Adv Enzym Regul* 3:425–438
- Hahl SK, Kremling A (2016) A comparison of deterministic and stochastic modeling approaches for biochemical reaction systems: on fixed points, means and modes. *Front Genet* 7(46):157
- Hasty J, Isaacs F, Dolnik M, McMillen D, Collins JJ (2001) Designer gene networks: towards fundamental cellular control. *Chaos (Woodbury, NY)* 11(1):207–220
- Janson NB (2012) Non-linear dynamics of biological systems. *Contemp Phys* 53(2):137–168
- Karpman VL, Sadvovskaya GV (1964) Oscillatory properties of the human body. *Bull Exp Biol Med* 55(6):649–652
- Kim J, Winfree E (2011) Synthetic in vitro transcriptional oscillators. *Mol Syst Biol* 7:465
- Kruse K, Jülicher F (2005) Oscillations in cell biology. *Curr Opin Cell Biol* 17(1):20–26
- Maini P (1996) Oscillations in biology. *Trends Biochem Sci* 21(10):403–403
- Maltoni M, Schwetz T, Tórtola M, Valle JWF (2004) Status of global fits to neutrino oscillations. *New J Phys* 6:1–37
- Purcell O, Savery NJ, Grierson CS, di Bernardo M (2010) A comparative analysis of synthetic genetic oscillators. *J R Soc Interface* 7(52):1503–1524
- Shaviv NJ, Prokoph A, Veizer J (2014) Is the solar system's galactic motion imprinted in the phanerozoic climate? *Sci Rep* 4:6150
- Simakov DSA, Pérez-Mercader J (2013) Noise induced oscillations and coherence resonance in a generic model of the nonisothermal chemical oscillator. *Sci Rep* 3:2404
- Singh V (2015) Modelling methodologies for systems biology. In: Singh V, Dhar PK (eds) *Systems and synthetic biology*. Springer, Dordrecht, pp 43–62. ISBN: 978-94-017-9513-5. <https://doi.org/10.1007/978-94-017-9514-2>

- Smolen P, Baxter DA, Byrne JH (1998) Frequency selectivity, multistability, and oscillations emerge from models of genetic regulatory systems. *Am J Phys* 274(2):531–542
- Stricker J, Cookson S, Bennett MR, Mather WH, Tsimring LS, Hasty J (2008) A fast, robust and tunable synthetic gene oscillator. *Nature* 456:516–519
- Tigges M, Marquez-Lago TT, Stelling J, Fussenegger M (2009) A tunable synthetic mammalian oscillator. *Nature* 457:309–312
- Tsimring LS (2014) Noise in biology. *Rep Prog Phys* 77(2):026601
- Winfree AT (2001) Populations of attracting-cycle oscillators. In: Winfree AT (ed) *The geometry of biological time*. Springer, New York, pp 229–257. ISBN: 978-0-387-98992-1. <https://doi.org/10.1007/978-1-4757-3484-3>
- Zeigler BP, Muzy A, Kofman E (2019) Introduction to systems modeling concepts. In: Zeigler BP, Kim TG, Praehofer H (eds) *Theory of modeling and simulation*. Academic Press, Orlando, pp 3–25. ISBN:978-0-12-778455-7. <https://doi.org/10.1016/C2016-0-03987-6>